Pits and adatoms at the interface of 1-ML C_{84}/Ag (111)*

Wang Peng(王 鹏)[a)b)], Zhang Han-Jie(张寒洁)[a)], Li Yan-Jun(李艳君)[a)], Sheng Chun-Qi(盛春荠)[a)], Li Wen-Jie(李文杰)[a)], Xing Xiu-Na(邢秀娜)[a)], Li Hai-Yang(李海洋)[a)], He Pi-Mo(何丕模)[a)], Bao Shi-Ning(鲍世宁)[a)], and Li Hong-Nian(李宏年)[a)†]

[a)] *Department of Physics, Zhejiang University, Hangzhou* 310027, *China*

[b)] *Department of Applied Physics, Shandong University of Science and Technology, Qingdao* 266590, *China*

(Received 6 June 2013; revised manuscript received 23 September 2013)

We prepare a well-defined C_{84} monolayer on the surface of Ag (111) and study the geometric structure by scanning tunneling microscopy (STM). The C_{84} molecules form a nearly close-packed incommensurate $R30°$ lattice. The lattice is long-distance ordered with numerous local disorders. The monolayer exhibits complex bright/dim contrast; the largest height difference between the molecules can be greater than 0.4 nm. Annealing the monolayer at 380 °C can desorb part of the molecules, but more than sixty percent molecules stay on the Ag (111) surface even after the sample has been annealed at 650 °C. Our analyses reveal that the 7-atom pits form beneath many molecules. Some other molecules sit at the 1-atom pits. Ag adatoms (those removed substrate atoms, accompanying the pit formation) play a very important role in this system. The adatoms can either stabilize or destabilize the monolayer, depending on the distribution manner of the adatoms at the interface. The distribution manner is determined by the co-play of the following factors: the dimension of the interstitial regions of the C_{84} overlayer, the number of the adatoms, and the long-distance migration of part adatoms.

Keywords: 1-ML C_{84}/Ag (111), geometric structure, pit, adatom, STM

PACS: 68.55.ap, 68.35.Ct, 68.37.Ef, 68.43.Hn **DOI:** 10.1088/1674-1056/22/12/126803

1. Introduction

The geometric structure of an adsorbate–substrate (A–S) system is the result of a delicate balance between the adsorbate–adsorbate (A–A) and A–S interactions. The fullerene (C_{60}, C_{70}, C_{84}, etc.) overlayer on a metal surface is especially interesting. Here, the A–A interaction is between charged molecules because of the charge transfer from metal to fullerene. The Coulomb repulsion between the charged molecules tends to expand the fullerene lattice; the lattice would collapse without the A–S interaction.[1] As a result, pits form at various fullerene/metal interfaces[1–11] to stabilize the overlayers. The role of the pit in stabilizing the molecular overlayer can be understood by facilitating the formation of as many as possible C–metal atom (C–M) bonds that have some covalent characteristics.[6,12] Accompanied with the pit formation, some metal atoms are dug out from the substrate and become so-called adatoms. The adatom may also be conducible to the stabilizing of a fullerene overlayer, as suggested theoretically.[13] Therefore, detailed knowledge about the pit and the adatom is indispensible to thoroughly understand the geometric structures of fullerene/metal systems.

Much progress has been achieved on the study of the pit. There are two pit configurations, namely the 1- and 7-atom pits (one and seven top-layer metal atoms removed by the adsorption of each molecule), formed at the (111) surfaces of transition and noble metals.[2,6,8–11] Other types of pits can form at more open surfaces, such as Ag (100) (4- or 5-atom pits)[7] and Pd (110) (8-atom pit).[5] In most cases, C_{60} digs a unique type of pit on one specific metal surface, but the C_{60}/Pd (110) interface is an exception where two types of pits seem to exist.[14] Two types of pit were also observed at the C_{70}/Ag (111) interface.[1] It was previously believed that all molecules have pits beneath them, provided that the sample is well annealed. Recent work,[15–17] however, revealed that part of the molecules had no pits beneath for well-annealed C_{60} monolayers on the surfaces of Ag (111) (1-ML C_{60}/Ag (111)) and Au (111) (1-ML C_{60}/Au (111)).

Knowledge about the adatom is rather limited as compared with that about the pit. A few studies revealed that the adatoms can insert beneath some molecules, resulting in multiple topographic contrasts for C_{60} on the surfaces of Ni (110),[3] Ni (111),[8] Ag (100),[18] and Cu (111).[19] In a theoretical study[13] on 1-ML C_{60}/Al (111), it was suggested that the Al adatoms filled in the interstitial regions of the C_{60} overlayer and helped to stabilize the overlayer at high temperatures up to 700 K. However, the adatoms have been ignored by the experimental analyses and density functional theory (DFT) calculations of the geometric structures for many other fullerene/metal systems up to this date. Considering the blocking of the overlayer, we believe that the adatoms cannot be desorbed from any fullerene/metal system and that only a very small part of the total adatoms can diffuse to the substrate edges for an ML sample where the substrate is fully covered by fullerenes. The effects of the adatoms on the geometric and

*Project supported by the National Natural Science Foundation of China (Grant Nos. 11079028 and 11374258).

†Corresponding author. E-mail: phylihn@public.zju.edu.cn

© 2013 Chinese Physical Society and IOP Publishing Ltd

electronic structures should be a universal and significantly important issue for all fullerene/metal systems.

In this paper, we report on a scanning tunneling microscopy (STM) study of the geometric structure of 1-ML C_{84}/Ag (111). As compared with C_{60} MLs, there has been very limited work of C_{84} MLs on metal surfaces.[20,21] We can anticipate some new information about the pit and the adatom considering the increased molecular size of C_{84} and the altered A–A and A–S interactions. Indeed, our sample shows a significant morphology change and novel desorption behavior (only part molecules desorbed) at high temperatures, from 310 °C to 650 °C. This offers a scarce and excellent opportunity for us to study the creation, migration and distribution of the adatoms, as well as the comprehensive effects on the geometry and stability of the fullerene overlayer. We also find that the 7-atom pit, which could not form at the C_{60}/Ag (111) interface,[12] widespreadly exists at the C_{84}/Ag (111) interface.

2. Experiment

Experiments were performed in an Omicron instrument for surface science at a base pressure better than 2.0×10^{-8} Pa. The C_{84} powder source was the commercial product (99% mixture of two isomers, BuckyUSA, Houston, TX, USA), which was thoroughly degassed and sublimed from a Ta boat located at about 11 cm from an Ag (111) substrate. The two isomers in the source were $D_2(22)$–C_{84} and $D_{2d}(23)$–C_{84} with a 2:1 abundance ratio. The history of identifying these isomers and the meaning of their notations can be found in Ref. [22] and the references therein. The clean and ordered surface of the Ag (111) single crystal was obtained by the standard Ar^+ sputtering and annealing procedure. The substrate was kept at room temperature during C_{84} deposition. We adopted a deposition rate of ∼0.05 ML/min to prepare C_{84} overlayers with various coverages. After the coverage reached ∼5 ML, we annealed the sample at 310 °C for 20 min to obtain 1-ML C_{84}/Ag (111). The ML sample was further annealed at 380 °C, 500 °C, and 650 °C (all for 20 min) to study the structural evolution. STM images were recorded at room temperature for each stage of the sample preparation history, but specially detailed measurements were carried out only on the sample annealed at 310 °C. The STM images were measured in the constant current mode using a chemically etched tungsten tip and the biases were referred to the sample. The heights of the atomic steps of the Ag (111) substrate were measured to be 0.23 nm–0.24 nm; thus the height values of the C_{84} overlayers should be rather accurate. Low-energy electron diffraction (LEED) was used to determine the crystallographic directions of the substrate and check the orientation of the C_{84} lattice for the sample annealed at 380 °C.

3. Results and discussion

3.1. Experimental observations

C_{84}-adopted island growth mode on the Ag (111) surface and the surface topography of the 5-ML sample was rather rough. After the annealing at 310 °C, we acquired the STM images shown in Fig. 1. Figures 1(a) and 1(b) show two representative images of the sample; figures 1(c) and 1(d) display line profiles. This sample had a layered structure, but it was an ML because the height differences (HDs) between the molecules were still much smaller than the molecular sizes (average diameters of 0.8133 nm and 0.8233 nm for $D_2(22)$–C_{84} and $D_{2d}(23)$–C_{84} respectively).[23] Many STM studies on C_{60} (with a diameter of 0.71 nm) have demonstrated that the HD between the second and the fist molecular layers is greater than 0.8 nm.[24,25]

We first analyze the in-plane packing of the molecules. Local-disorders can be frequently observed. The ellipse in Fig. 1(a) points out a dislocation. Upon close inspection of the Fig., one can find that even those molecular chains far from the dislocation are not strict straight lines (see the molecules highlighted by a dashed rectangle). The local-disorders are also reflected on the line profiles. The inter-molecular distance measured in a small region (several molecules) is not a constant. However, from a long-distance view, all molecules are arranged in a close-packed lattice, as indicated by the hexagon in Fig. 1(a). The long-distance order has not been observed previously for C_{84} MLs on the surfaces of Au (111)[20] and Si (100) 2×1.[21] The rotational angle of the C_{84} lattice is 30° with respect to the $[\bar{1}01]$ direction of the Ag (111), i.e., the molecular chain aligns along the $[\bar{1}\bar{1}2]$ direction. We did not find any other rotational angle by a large amount of scanning on a great many areas of the sample. The averaged nearest-neighbor distances (NNDs) of the molecules as measured on large distance scales (greater than 15 molecules) in different sample regions, are rather coincident and amount to 1.13 nm–1.14 nm. These observations reveal that the C_{84} lattice is incommensurate with the substrate because the first-order commensurate structure corresponding to the rotational angle of 30° is the $(2\sqrt{3} \times 2\sqrt{3})R30°$ structure. This commensurate structure requires a molecular NND of 1.001 nm (the atomic distance is 0.289 nm for Ag (111) surface[26]), far from the 1.13 nm–1.14 nm observed here. The local disorders further preclude the possibility of higher-order commensurate structures. So we say that the 1-ML C_{84}/Ag (111) has an incommensurate, long-distance ordered, and close-packed $R30°$ structure with numerous local-disorders.

Then we turn our attention to the out-of-plane bright/dim (B/D) contrast. Most areas of the sample present a double-layer structure with exceptionally few isolated extremely bright molecules (EBMs); figure 1(a) shows a representative of these areas. The brightness of one EBM in the top-right of the

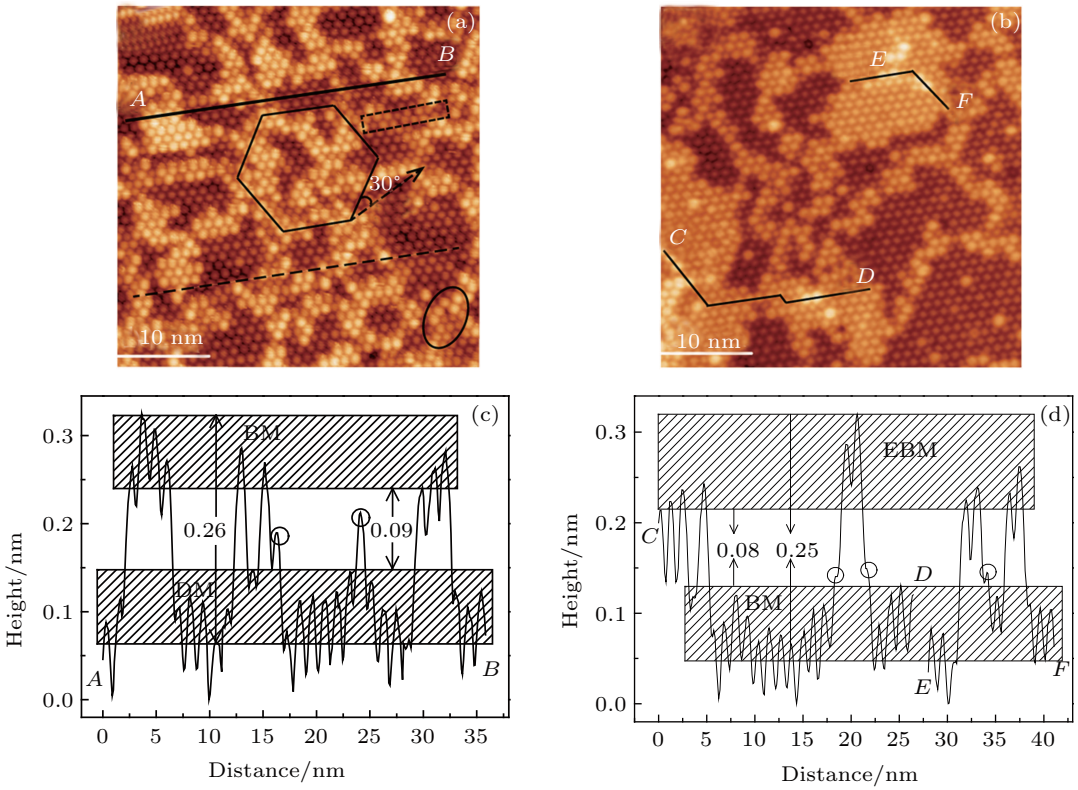


Fig. 1. (color online) Representative STM images of the 1-ML C_{84}/Ag (111). (a) Region of double-layer with very few extremely bright molecules (40×40 nm, $V = -0.76$ V, $I = 0.36$ nA). The hexagon highlights the close-packing of the molecules. The ellipse helps one to see a dislocation and the dashed rectangle indicates the distribution of some molecules departing from strict straight lines. The $[\bar{1}01]$ direction of the substrate is indicated by a dashed arrow. (b) Region of triple-layer (40×40 nm, $V = -1.0$ V, $I = 0.20$ nA). (c) A line profile along *AB*. (d) Line profiles along paths *CD* and *EF*.

figure has been truncated to highlight the B/D contrast of the lower double-layer. One may consider the EBM as an impurity. However, the B/D contrast like that shown in Fig. 1(b) is not rare in the sample. In Fig. 1(b), the number of EBMs is not too small. Many of the EBMs are adjacent to each other, forming chains or small islands. The observed adjacent distribution of the EBMs precludes the possibility of an impurity. We are thus faced with a C_{84} ML with double-layer and triple-layer structures. Note that the nomenclatures of the double- and triple-layer do not mean a molecular layer. Rather, they mean three groups of heights of one molecular layer. The line profiles in Figs. 1(c) and 1(d) more clearly display the three groups of heights. Figure 1(c) shows the comparison between the heights of the dim molecules (DMs) and the bright molecules (BMs); figure 1(d) displays the comparison between heights of the BMs and the EBMs. There are distinct height gaps (0.08 nm–0.09 nm) between these groups except for a few exceptions (those circled peaks). The heights in each group are rather dispersive. The dispersion is, however, smaller than 0.08 nm for groups DM and BM and smaller than 0.11 nm for group EBM. The largest HD between the EBM and the DM is ∼0.4 nm.

Figure 2 shows an STM image and the LEED pattern of the sample annealed at 380 °C. The LEED pattern in Fig. 2(b) reveals a unique close-packed lattice rotated by 30° as compared with that of the clean Ag (111) (the LEED pattern of the clean Ag (111) was measured with an incident electron energy of 118 eV, which is not shown here), coincident with the rotational angle of 30° observed in Fig. 1. The NND and the HD as measured by the STM scanning in some small regions (< 50 nm), are also coincident with the results from Fig. 1. The large range STM image (Fig. 2(a), 200×200 nm) and the line profiles (Fig. 2(c)) show some new observations. Firstly, part of the molecules desorbed and left behind regions of bare Ag (111). Secondly, the average height of the DMs is ∼0.5 nm with respect to the Ag (111), much smaller than the molecular sizes.[23] Thirdly, the number of the BMs substantially decreased and many large regions (hundreds of square nanometers in area) contained exclusively the DMs. Lastly, very occasionally, two very bright spots (each has several molecules) emerge with a height greater than the surrounding molecules by ∼0.74 nm.

The areas of the exposed parts of the Ag (111) substrate increased gradually with the increase of annealing temperature. However, our STM scanning in many large regions ($\geq 200 \times 200$ nm) revealed that greater than sixty percent of the C_{84} molecules still stayed on the Ag (111) surface even after the sample had been annealed at 650 °C. Figure 3(a) shows a 300×300 nm image of the sample annealed at 650 °C. The remaining C_{84} overlayer became rather rugged. This is not surprising because the Ag (111) surface became unstable at such high temperatures (450 °C is already sufficiently high

enough to produce a satisfactory clean Ag (111) surface in the Ar^+ sputtering and annealing procedure). Therefore, we do not discuss the detailed morphologies of the samples annealed at 500 °C and 650 °C in this work. A small range STM image is shown in Fig. 3(b) to state that the C_{84} molecules are intact (not decomposed) and not polymerized, even at 650 °C. The HD between the BMs and the DMs in Fig. 3(b) is ∼0.18 nm.

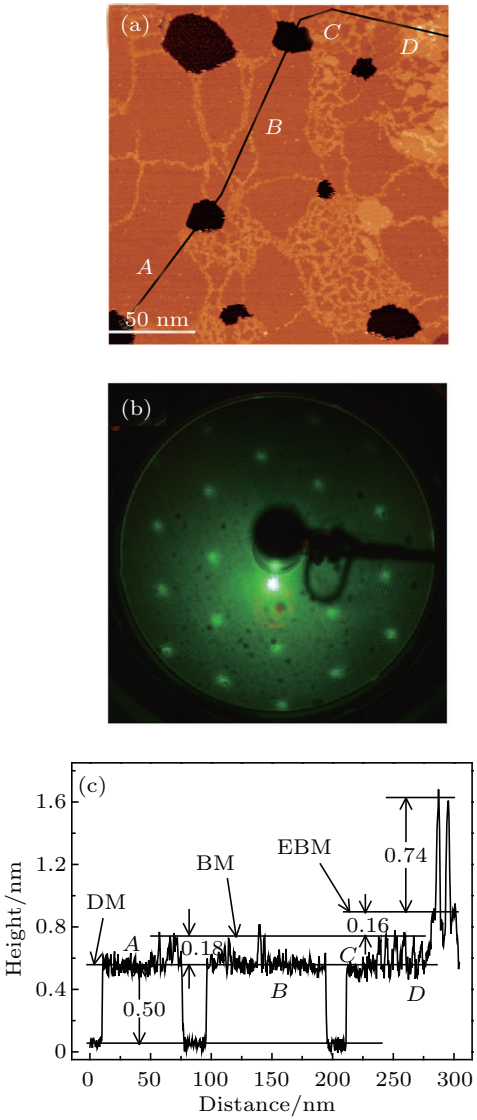


Fig. 2. (color online) (a) STM image (200 × 200 nm, $V = -0.75$ V, $I = 0.20$ nA) of the sample annealed at 380 °C. Many areas of bare Ag (111) emerge. (b) LEED pattern measured with an incident electron energy of 19 eV. (c) Line profiles along the path (*ABCD*) indicated in panel (a).

The increased areas of the exposed parts of the Ag (111) substrate prompted us to find some direct evidence of the pits. Figure 3(c) shows many dark spots on the bare Ag (111) of the sample annealed at 500 °C. These dark spots were never observed on the clean Ag (111), but could be frequently seen on the samples annealed at 500 °C and 650 °C. We did not perform detailed measurements for the bare Ag (111) nor for small regions ($\leq 50 \times 50$ nm) containing bare Ag (111) for the sample annealed at 380 °C, but some images of 100 nm × 100 nm size indeed also presented blurred black spots on the bare Ag (111). The dark spots should correspond to the pits. We believe that we have for the first time directly observed the pits at the fullerene/metal interface. This is due to the desorbed C_{84} molecules and also to the remaining molecules that hindered some Ag atoms from freely diffusing at the C_{84}/Ag (111) interface to fill the observed pits. There should be, of course, some other pits that have been filled; the dark spots in Fig. 3(c) do not necessarily characterize the shape and depth of the pristine pits.

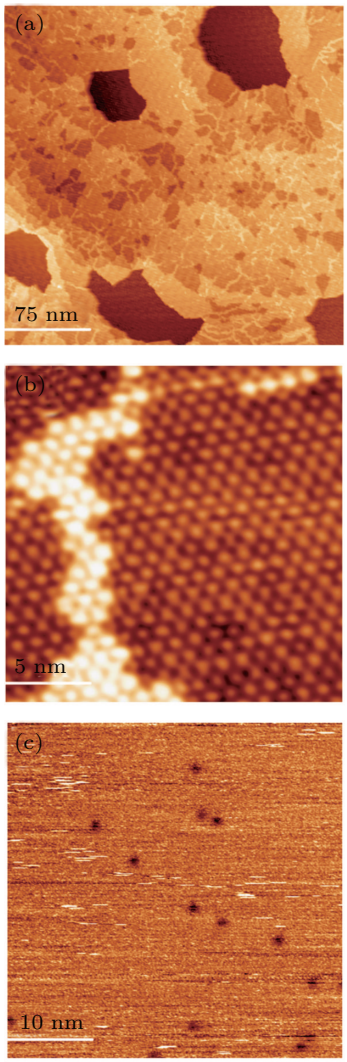


Fig. 3. (color online) (a) STM image (300 × 300 nm, $V = -1.5$ V, $I = 1.0$ nA) of the sample annealed at 650 °C. (b) STM image (20 × 20 nm, $V = -0.76$ V, $I = 0.21$ nA) showing the integrity of the C_{84} molecules after the sample has been annealed at 650 °C. (c) STM image (40 × 40 nm, $V = -1.4$ V, $I = 3.0$ nA) of the exposed Ag (111) substrate measured on the sample annealed at 500 °C.

3.2. Discussion

In this section, we try to understand the B/D contrast in Figs. 1 and 2 and the desorption behavior up to 650 °C. In Subsection 3.2.1, we analyze the B/D contrast between the BMs and the DMs. Then the desorption behavior is discussed in

Subsection 3.2.2. The discussion of the B/D contrast related to the EBMs has to be postponed to the end of Subsection 3.2.2 due to a lack of sufficient knowledge about the interface before we can understand the desorption behavior.

3.2.1. Pit configuration

The B/D contrast cannot be induced by the two types of isomers in the sample because the number ratio of B molecules to D molecules is temperature-dependent (not a constant of 2:1 or 1:2, corresponding to isomer abundance). Actually, the sizes and shapes of $D_2(22)$–C_{84} and $D_{2d}(23)$–C_{84} are rather similar (the long, middle, and short axes are 0.845, 0.816, and 0.779 nm for $D_2(22)$–C_{84} and 0.850, 0.830, and 0.790 nm for $D_{2d}(23)$–C_{84}).[23] Their electronic structures are also similar.[27] We cannot expect to discriminate between them by STM measurements at room temperature.

Molecular orientation should be one of the reasons for the B/D contrast. Different molecular orientations can at most result in an HD of 0.071 (= 0.850–0.779) nm, which may be responsible for a height dispersion of ∼0.8 nm within groups BM and DM. However, the molecular orientation cannot explain the height gap between the BMs and the DMs. The distinct height gap and the large difference between the average height of the BMs and the DMs (∼ 0.18 nm, Fig. 2(c)) can be interpreted only with the pits formed at the C_{84}/Ag (111) interface. The DMs must sit at the pits, since their average height is as small as ∼0.5 nm. There are two possibilities for the BMs. They are either adsorbed on the unreconstructed parts of the substrate or sit at other types of pits shallower than those beneath the DMs.

To thoroughly understand the B/D contrast, we should make clear the pit configurations. This is a challenging task because STM cannot directly measure the metal surface beneath the molecules. In the following, we put forward some seemingly reasonable suggestions of the pit configurations from a physical point of view and test the suggestions by using the measured data of the HDs.

At the present stage of scientific knowledge, the number of the covalent (or near-covalent) C–M bonds allowed by one specific pit configuration is a measure of its stability.[6,12] So we suggest that 7-atom pits exist at the C_{84}/Ag (111) interface. Figure 4 illustrates the possible 7-atom pit configuration in which seven top-layer Ag atoms beneath a molecule are dug out. This Fig. was depicted with the three-dimensional (3D) viewer of the Materials Studio software; the C–C and Ag–Ag distances are proportional to their actual values. We placed a $D_{2d}(23)$–C_{84} (geometrically optimized with the CASTEP package[28] implemented in the Materials Studio) at the atop position with the six-member ring facing down. The six-member ring is assumed to be coplanar with the top-layer Ag atoms, in accordance with the experimentally determined case for C_{60} in a 7-atom pit (1-ML C_{60}/Cu (111)).[29] By manually rotating the molecule around the surface normal, we obtained a configuration that has strong bonds between 15 C atoms and 9 Ag atoms. We say that these bonds are strong because the bond lengths are 0.231 nm–0.240 nm, near the sum of the covalent radii of C and Ag (0.221 nm[26]). As a comparison, some C–Cu bonds with lengths of 0.223 nm–0.229 nm were considered as strong near-covalent bonds for the well-known 7-atom pit at the interface of C_{60}/Cu (111)[29] (the sum of the covalent radii of C and Cu is 0.208 nm[26]). So, the many near-covalent bonds in Fig. 4 indicate that the 7-atom pit is preferable at the C_{84}/Ag (111) interface.

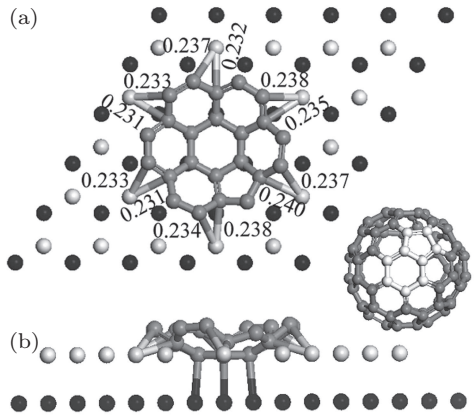


Fig. 4. (a) Illustration of the nearest C–Ag distances for a D_{2d}–C_{84} sitting at a 7-atom pit. Only the 23 C atoms (in grey) that are nearest the substrate are shown. The light grey and black balls represent the top and second atomic layers of the Ag (111), respectively. Seven top-layer Ag atoms beneath the molecule have been removed; the Ag lattice is assumed to be undistorted by the adsorbate. (b) Side view of (a) exhibiting the C–Ag distances between the three bottom C atoms and three second-layer Ag atoms. The size of the molecule and the atomic distance of the Ag (111) are proportional to their actual values in panels (a) and (b). The white-colored C atoms in the inset indicate the supposed molecular orientation and the six-member ring intimately contacting the Ag (111). See the text for more details.

Shi *et al.*[12] revealed that the number of near-covalent C–M bonds was determined by the substrate geometric structure (including the surface lattice constant and the interlayer spacing). The illustrations in Fig. 4 reveal that molecular size is another factor in determining the pit configuration. If we put a smaller molecule, such as C_{60}, into the 7-atom pit of the Ag (111) surface, the dimension of the pit is too large for C_{60} to form so many near-covalent bonds, as in the case of Fig. 4. In other words, the 7-atom pit is not a stable adsorption structure for C_{60}/Ag (111). Indeed, C_{60} digs the 1-atom pit on the Ag (111) surface.[9,17]

The 7-atom pits need a large formation energy. If the annealing temperature is not high enough or the annealing time is not long enough, we can anticipate the 1-atom pit as the precursor at the C_{84}/Ag (111) interface.

So we suggest that the DMs (or most of the DMs) in Figs. 1 and 2 sit at the 7-atom pits, while the BMs (or part

of BMs) sit at the 1-atom pits. The HDs shown in Fig. 1(c) support this suggestion. According to some DFT calculations of C_{60}/metal systems,[9,30,31] the vertical separations between the bottom of C_{60} and the top-layer of Au (111) or Ag (111) (Au and Ag have nearly identical lattice constants[26]) are 0.229, 0.180, and 0.015 nm for an unreconstructed substrate, a 1-atom pit and a 7-atom pit, respectively. We can apply these DFT results to the C_{84}/Ag (111) system with minor error (the separations may change somewhat when C_{60} is substituted by C_{84}, but the changes should be small). Different (1-atom or 7-atom) pit configurations result in an HD of 0.165 $(= 0.180 - 0.015)$ nm. The molecular orientations result in an HD of 0.071 nm, as mentioned above. Summing up, the two types of HDs gives the largest HD, which amounts to 0.236 $(= 0.165 + 0.071)$ nm, near to the measured value of 0.26 nm in Fig. 1(c). Subtracting the two types of HDs gives a height gap of 0.094 $(= 0.165 - 0.071)$ nm, showing good coincidence with the value of 0.09 nm in Fig. 1(c).

However, we do not preclude the possibility of some BMs from being adsorbed on the unreconstructed substrate (not having pits beneath). These molecules can relieve the in-plane stress of the C_{84} overlayer if they are dispersed among other types of molecules. Actually, the slight disagreement (0.236 nm versus 0.26 nm) in our interpretation of the largest HD implies that some BMs have no pit beneath. The measured (apparent) height is not the actual height due to the electronic contribution to the STM image. Figures 1 and 2 were measured with the samples negatively biased (–0.75, –0.76 and –1.0 V), corresponding to the electrons tunneling from the lowest unoccupied molecular orbital (LUMO) of C_{84} to the tip. The pit can enhance the charge transfer from the metal to the LUMO of fullerene.[10] A deeper pit facilitates more electrons occupying the LUMO and increases the apparent height of the molecule. That is to say, the electronic contribution from different pit configurations is to reduce (rather than overestimate) the apparent HD between the molecules. Considering this fact, the actual HD should be greater than 0.26 nm. If we assume some B molecules have no pits beneath them, the HD between these BMs and the D molecules should be increased by 0.049 $(= 0.229 - 0.180)$ nm. Then the largest HD becomes 0.285 nm, reasonably greater than the measured value of 0.26 nm.

We cannot even preclude the possibility of some other types of pits from emerging at the C_{84}/Ag (111) interface. This is because one molecule, when one or more nearest-neighbor molecules have already been adsorbed on the atop positions, cannot also sit at an atop position due to the incommensurate C_{84} lattice. Some other adsorption sites may facilitate the formation of other types of pits. Those exceptional molecules circled in Fig. 1(c) may sit at, say, the 3- or 4-atom pits. The number of other types of pits should be small, as indicated by the distinct height gap (very few exceptional molecules). The interface could distort somewhat to facilitate the formation of as many as 7-atom pits, in principle, as many as possible; we suggest that this is one of the reasons for the local-disorders observed in Fig. 1.

Thus far, we have successfully interpreted the B/D contrast between the BMs and the DMs with the suggestions of the 7-atom pits, the 1-atom pits and some unreconstructed regions of the substrate. The desorption behavior can also be understood based on these suggestions, as discussed in the next subsection.

3.2.2. Adatom

We now consider the morphology evolution and the desorption behavior of the C_{84} overlayer. We previously suggested that the 1-atom pit acted as the precursor of the 7-atom pit. However, Figs. 1–3 reveal that the more stable 7-atom pit adsorption structure does not prohibit some molecules from still sitting at the 1-atom pits (or on the unreconstructed parts of the substrate) at high temperatures. The number of the BMs indeed decreased in Fig. 2 due to the fact that the annealing of the sample at 380 °C affords the energy for the formation of more 7-atom pits, but some BMs survived even at 650 °C (Fig. 3). What is the reason for the stability of the remaining BMs? Actually, even the DMs in Figs. 2(a) and 3(b) need justification beyond the interpretation of the many near-covalent bonds, as depicted in Fig. 4. Some molecules have already been desorbed at 380 °C. The desorbed molecules cannot merely be those BMs or EBMs. Rather, some DMs previously observed in Fig. 1 are also desorbed, because the areas of the bare Ag (111) in Fig. 2 (and on the samples annealed at 500 °C and 650 °C) were surely once covered by some DMs.

We suggest that the Ag adatoms play an important role here. We consider those large regions (hundreds of square nanometers in area) of exclusive DMs in Fig. 2(a). If no pits exist, there were ∼15.3 top-layer Ag atoms beneath each C_{84} molecule, according to the NND of the C_{84} lattice (1.13 nm) and the atomic distance (0.289 nm) of the Ag (111) surface. After the formation of the 7-atom pits, about 46% (≈7/15.3) of the top-layer Ag atoms were dug out and became the adatoms. The adatoms must obtain their accommodations. The illustrations in Figs. 5(a) and 5(c) reveal that the interstitial regions of the C_{84} overlayer have sufficient room to accommodate these adatoms. In Figs. 5(a) and 5(c), we placed three C_{84} molecules on the unreconstructed Ag (111) surface with one six-member ring of each molecule facing down and being coplanar with the top-layer Ag atoms (we do not consider the possibilities of a five-member ring or a C–C bond facing down in this work, since experimental results have demonstrated that C_{60} has a six-member ring facing down in various pit configurations). Each molecular pair is arranged along the $\langle \bar{1}\bar{1}2 \rangle$ direction of the substrate; the distance between the centers of the bottom six-member rings is 1.13 nm. With this

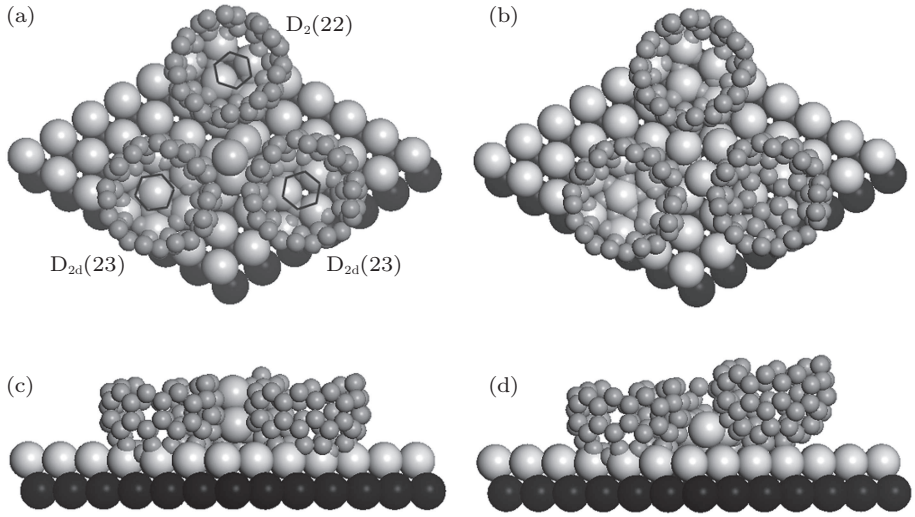


Fig. 5. Illustrations of the interstitial region of the C_{84} lattice offering enough room to accommodate the Ag adatoms: (a) top view of an Ag trimer staying in the interstitial region with the nearest C–Ag distances of 0.220 nm–0.240 nm. Three small hexagons denote the bottom six-member rings and indicate the molecular orientations. (b) An Ag trimer lying in another type of interstitial site where a C_{84} molecule (the bottom-right one) is sitting at a 1-atom pit. (c) and (d) are the side views of panels (a) and (b) respectively. The distances between the adatoms and the substrate atoms are no less than 0.289 nm. Upper parts of the molecules have been cut for clarity. See the text for more details.

configuration, an Ag trimer can stay in the interstitial region. The atomic distance of the trimer is 0.289 nm (equal to that of the Ag (111)); the nearest adatom–substrate distance is no less than 0.289 nm. Sufficient room can be directly perceived because we depicted the Figs. with the radii of the C and Ag atoms proportional to their covalent radii and proportional to the atomic distance of the Ag (111). Six of the seven adatoms for a 7-atom pit thus obtain their residence. Another adatom can be distributed in the interstitial region formed by the upper parts (cut in the Figs. for clarity) of the molecules. This filling manner can greatly enhance the stability of the C_{84} overlayer because the adatoms form the near-covalent bonds with the surrounding molecules (the nearest C–Ag distances between the trimer and the surrounding molecules are 0.220 nm–0.240 nm in Fig. 5(a)) and combine the molecules together. Besides, there should be some charge transferred from the adatoms to C_{84}. The charge transfer results in the Madelung effect that can also stabilize the overlayer. It was the adatoms that helped the DMs to stay on the Ag (111) surface above 380 °C.

Some other molecular orientations may reduce the interstitial volume. However, we need not worry about the case of an interstitial region too small to accommodate three adatoms. Figure 5 has reserved sufficient space by retaining all the top-layer Ag atoms and depicting two $D_{2d}(23)$–C_{84} molecules. Seven Ag atoms beneath each C_{84} molecule are removed in actual samples, which should afford a larger interstitial volume than that in Fig. 5. The abundance ration of the C_{84} isomers is $D_2(22)/D_{2d}(23)$ = 2:1, rather than the case in Fig. 5. $D_{2d}(23)$–C_{84} is slightly larger than $D_2(22)$–C_{84}; we deliberately depicted two $D_{2d}(23)$–C_{84} molecules to more severely test our suggestion. In addition, we supposed in Fig. 5 that the three adatoms are in the form of an equilateral triangle. The practical situation does not necessarily comply with the equilateral triangle; thus, three adatoms can even fill into a smaller interstitial region than that in Fig. 5(a).

The adatoms can also stabilize the BMs. The volume of the interstitial region encompassed by three molecules can greatly increase when one or more molecules sit at the 1-atom pits or have no pits underneath. Figures 5(b) and 5(d) illustrate the case of one molecule sitting at the 1-atom pit (the right molecule in Fig. 5(b) is lifted by 0.165 nm in Fig. 5(d)). The Ag trimer can now lie down with redundant room. More adatoms can then enter into the interstitial region. There are two ways for the subsequent adatoms to enter into the interstitial region. One is that another adatom enters into the interstitial region of Fig. 5(b) and forms a Ag tetramer with the existing trimer. There is sufficient room to accommodate the fourth adatom in Figs. 5(b) and 5(d) (not shown for clarity); more than four adatoms could fill the interstitial region if more molecules sit at the 1-atom pits or the molecules have no pit beneath. In this way, the BMs are stabilized, in analogy with the case of Fig. 5(a). So we can still observe the BMs in Figs. 2(a) and 3(b). Of course, stabilizing the BMs requires a sufficient number of adatoms that cannot be afforded locally by the 1-atom pit or unreconstructed Ag (111). Otherwise the BMs would be desorbed at high temperatures, which has already been observed on the sample annealed at 380 °C. One source of the required adatoms is that produced by the 7-atom pits. As mentioned previously, one of every seven adatoms is distributed in the interstitial region formed by the upper parts of the DMs; this adatom can easily diffuse in the C_{84} lattice at high temperatures. Another source may be the adatoms left behind by the desorbed molecules. Some of these adatoms could diffuse into the C_{84} lattice although most of them should refill the pits.

The mechanisms of the stability of the DMs and the BMs can satisfactorily interpret the morphology evolution and the desorption behavior of the C_{84} overlayer. The number of BMs is no less than that of the DMs in Fig. 1. After the sample was annealed at 380 °C, the number of DMs increased substantially due to the formation of more 7-atom pits facilitated by the higher temperature affording the pit formation energy. Meanwhile, some BMs had been desorbed before they were converted into DMs or obtained a sufficient number of adatoms to stabilize them. Some DMs, if they were adjacent to the desorbed BMs, also had some probability to be desorbed because one side of these DMs does not have a sufficient number of adatoms and loses the in-plane constraint by other molecules. After the desorption of some molecules and the formation of more 7-atom pits, the number of the available adatoms increased. More molecules could obtain a sufficient number of adatoms to bear the annealing at higher temperatures. Of course, there should still be some molecules that do not have sufficient adatoms nearby and desorbed by the annealing at 500 °C and 650 °C, interpreting the gradually increased area of the exposed Ag (111). The required adatoms are produced locally for the DMs; thus we can observe large regions of exclusive DMs in Fig. 2(a). On the other hand, it is difficult to form large patches of exclusive BMs above 380 °C because most of the required adatoms have to be obtained through the long-distance migration of those adatoms created elsewhere.

Another way for a subsequent adatom to enter into the interstitial region of Fig. 5(b) is that the adatoms grow into small island in the plane of the trimer and are inserted beneath the BMs, which is responsible for the EBMs observed in Fig. 1 and the top-right region of Fig. 2(a). After being inserted with the atomic island, the BM raises its height and becomes the EBM. The island beneath the EBM is not necessarily as compact a lattice as the clean Ag (111). Owing to the constraint of the number of the available adatoms, atomic deficiency may be produced underneath an EBM or the island is not large enough to insert the entire region below an EBM. So the average height of the EBMs in Figs. 1 and 2 is higher than the BMs by less than an atomic step (0.235 nm) of the Ag (111) and the dispersion of the height (∼0.11 nm in Fig. 1(d)) is greater than those of the BMs and DMs. Those exceptional BMs circled in Fig. 1(d) may correspond to the case of very few adatoms inserted beneath. The probability of growing an island (rather than crowding in the interstitial region) would increase in some sample regions where many adjacent molecules sit at the 1-atom pits (or have no pit underneath) and thus expand to a large interstitial volume as compared with the case in Fig. 5(b). So the EBMs are generally observed surrounded by the BMs. The EBMs are obviously the most unstable and the premier desorbed molecules. The easy desorption of the EBMs may be another important reason for the desorption of some BMs and DMs at 380 °C. With the molecular vacancies resulting from the desorption of the EBMs, the in-plane constraint of the C_{84} monolayer weakened and some BMs and DMs became easy to be desorbed. We can still observe the EBMs in Fig. 2(a) because their emerging is a dynamic process. Some EBMs are desorbed while some new EBMs are produced. The very bright (∼0.74 nm higher than the surrounding EBMs) molecules in the top-right of Fig. 2(a) may be those newly-formed EBMs just about to be desorbed but hindered by the low sample temperature during sample cooling (from 380 °C to room temperature for STM measurements). This distribution manner (island) of the adatoms helps to decompose the C_{84} overlayer. The adatoms left behind by the desorbed EBMs, if they diffuse as a whole and are inserted beneath other molecules, can also decompose the C_{84} overlayer. If these adatoms are dispersed, they, on the contrary, will help to stabilize the sample.

At the end of this section, we state that our suggestions of the adatoms can help to understand the different desorption behaviors of 1-ML C_{60}/Ag (111) and 1-ML C_{70}/Ag (111), as compared with the case of the 1-ML C_{84}/Ag (111). C_{60} or C_{70} monolayers were kept intact at 410 °C[9] or 380 °C,[1] but almost all the molecules on the terraces of the Ag (111) surface were desorbed at 500 °C.[1,24] The pits at the C_{60}/Ag (111) interface were the 1-atom pits[9,17] and the pits at the C_{70}/Ag (111) interface were predominantly the 1-atom pits with very few 7-atom pits.[1] So the number of adatoms was insufficient to help to stabilize the molecular layers at 500 °C. The insufficient number of adatoms, on the other hand, prevented the molecules from becoming the EBMs; thus no C_{60} or C_{70} molecules were desorbed at 380 °C.

4. Conclusions

The 1-ML C_{84}/Ag (111) has a near close-packed incommensurate $R30°$ structure. The structure is long-distance ordered with a lattice constant of 1.13 nm–1.14 nm. The C_{84} monolayer exhibits three groups of apparent heights. Annealing at high temperatures can desorb some molecules, but many molecules stayed on the Ag (111) surface even after the sample has been annealed at 650 °C. To understand our experimental observations, we have put forward some suggestions about the reconstruction of the substrate (the 1- and 7-atom pits) and the distribution manner of the adatoms (filling in the interstitial regions or inserting beneath the molecules). These suggestions, though they need to have more direct support experimentally or theoretically, seem to be reasonable and generally correct because they can excellently interpret the complicated morphology and the novel desorption behavior of 1-ML C_{84}/Ag (111).

References

[1] Wang P, Zhang H J, Li Y J, Sheng C Q, Shen Y, Li H Y, Bao S N and Li H N 2012 *Phys. Rev. B* **85** 205445

[2] Maxwell A J, Brühwiler P A, Andersson S, Arvanitis D, Hernnäs B, Karis O, Mancini D C, Mårtensson N, Gray S M, Johansson M K J and Johansson L S O 1995 *Phys. Rev. B* **52** R5546

[3] Murray P W, Pedersen M Ø, Lægsgaard E, Stensgaard I and Besenbacher F 1997 *Phys. Rev. B* **55** 9360

[4] Pedio M, Felici R, Torrelles X, Rudolf P, Capozi M, Rius J and Ferrer S 2000 *Phys. Rev. Lett.* **85** 1040

[5] Weckesser J, Barth J V and Kern K 2001 *Phys. Rev. B* **64** R161403

[6] Felici R, Pedio M, Borgatti F, Iannotta S, Capozi M, Ciullo G and Stierle A 2005 *Nat. Mater.* **4** 688

[7] Zhang X Q, He W, Zhao A D, Li H N, Chen L, Pai W W, Hou J G, Loy M M T, Yang J L and Xiao X D 2007 *Phys. Rev. B* **75** 235444

[8] Lin C H, Lin K C, Tang T B and Pai W W 2008 *J. Nanosci. Nanotechnol.* **8** 602

[9] Li H I, Pussi K, Hanna K J, Wang L L, Johnson D D, Cheng H P, Shin H, Curtarolo S, Moritz W, Smerdon J A, McGrath R and Diehl R D 2009 *Phys. Rev. Lett.* **103** 056101

[10] Gardener J A, Briggs G A D and Castell M R 2009 *Phys. Rev. B* **80** 235434

[11] Pai W W, Jeng H T, Cheng C M, Lin C H, Xiao X D, Zhao A D, Zhang X Q, Xu G, Shi X Q, Van Hove M A, Hsue C S and Tsuei K D 2010 *Phys. Rev. Lett.* **104** 036103

[12] Shi X Q, Van Hove M A and Zhang R Q 2012 *Phys. Rev. B* **85** 075421

[13] Stengel M, De Vita A and Baldereschi A 2003 *Phys. Rev. Lett.* **91** 166101

[14] Weckesser J, Cepek C, Fasel R, Barth J V, Baumberger F, Greber T and Kern K 2001 *J. Chem. Phys.* **115** 9001

[15] Chen W, Zhang H L, Huang H, Chen L and Wee A T S 2008 *ACS Nano* **2** 693

[16] Tang L, Xie Y and Guo Q 2011 *J. Chem. Phys.* **135** 114702

[17] Pussi K, Li H I, Shin H, Serkovic Loli L N, Shukla A K, Ledieu J, Fournée V, Wang L L, Su S Y, Marino K E, Snyder M V and Diehl R D 2012 *Phys. Rev. B* **86** 205406

[18] Pai W W and Hsu C L 2003 *Phys. Rev. B* **68** R121403

[19] Pai W W, Hsu C L, Lin M C, Lin K C and Tang T B 2004 *Phys. Rev. B* **69** 125405

[20] Guo S, Nagel P M, Deering A L, Van Lue S M and Alex Kandel S 2007 *Surf. Sci.* **601** 994

[21] Wang X D, Hashizume T, Shinohara H, Saito Y, Nishina Y and Sakurai T 1993 *Phys. Rev. B* **47** 15923

[22] Wang P, Ni J F, Meng L, Wang X B, Sheng C Q, Zhang W H, Xu Y, Xu F Q, Zhu J F and Li H N 2012 *Carbon* **50** 1762

[23] Margadonna S, Brown C M, Dennis T J S, Lappas A, Pattison P, Prassides K and Shinohara H 1998 *Chem. Mater.* **10** 1742

[24] Altman E I and Colton R J 1993 *Surf. Sci.* **295** 13

[25] Hashizume T, Motai K, Wang X D, Shinohara H, Saito Y, Maruyama Y, Ohno K, Kawazoe Y, Nishina Y, Pickering H W, Kuk Y and Sakurai T 1993 *Phys. Rev. Lett.* **71** 2959

[26] Lide D R 2007 *CRC Handbook of Chemistry and Physics* (Boca, Raton, FL: Taylor and Francis, Florida, 2007) Internet Version

[27] Li H N, Yang H, Wang X X, Ni J F, Wang P, Meng L, Wang X B, Kurash I, Qian H J, Wang J O and Liu Z Y 2009 *J. Phys.: Condens. Matter* **21** 265502

[28] Segall M D, Lindan P J D, Probert M J, Pickard C J, Hasnip P J, Clark S J and Payne M C 2002 *J. Phys.: Condens. Matter* **14** 2717

[29] Xu G, Shi X Q, Zhang R Q, Pai W W, Jeng H T and Van Hove M A 2012 *Phys. Rev. B* **86** 075419

[30] Wang L L and Cheng H P 2004 *Phys. Rev. B* **69** 165417

[31] Tang L, Zhang X, Guo Q, Wu Y N, Wang L L and Cheng H P 2010 *Phys. Rev. B* **82** 125414